Korean J. Chem. Eng., 39(2), 306-315 (2022)
DOI: 10.1007/s11814-021-0908-z

pISSN: 0256-1115
eISSN: 1975-7220

Study on mass transfer and heat transfer in transition zone of short-path distillation separation equipment based on N-dodecanol and N-hexadecanol

Zhenya Duan*, Haodong Zhang*, Bin Liu*, Zhiwei Sun*, Junmei Zhang,†, and Longlong Lin*****

*College of Electromechanical Engineering, Qingdao University of Science and Technology, Qingdao 266061, China
**College of Chemical Engineering, Qingdao University of Science and Technology, Qingdao 266042, China
***Shandong Xinhua Pharmaceutical Company Limited, Zibo 255000, Shandong Province, China
(*Received 19 March 2021 • Revised 24 June 2021 • Accepted 20 July 2021*)

Abstract−Based on the fact that the distance between the heat exchange surfaces has little influence on the separation efficiency in the short-path distillation, a hypothesis that the heat and mass transfer process in the transition region is controlled by heat convection is proposed; the gas-liquid state in the transition zone was calculated by numerical simulation experiment. The results show that the gas-liquid volume fraction and temperature fluctuation in the evaporation and condensation process is unstable, while the gas-liquid volume fraction and temperature fluctuation in the transition zone is stable in the short-path distillation process. It can be concluded that in unsteady thermodynamics, the transition zone is a stable convective heat transfer process that is not affected by the distance between heat transfer surfaces. Thus, under ideal conditions, the continuous extension of the transition region has little effect on the distillation efficiency.

Keywords: Short-path Distillation, Fluent, Molecular Dynamic Simulation, Transition Region, Evaporation and Condensation

BACKGROUND AND INTRODUCTION

Molecular distillation, as an emerging technology suitable for the separation of high boiling point, heat-sensitive, and easily oxidized material, has been recognized as the safest separation and purification method [1,2]. It takes advantage of the difference between the critical boiling point of different substances (0-100 Pa) and the average free path of molecules under the vacuum condition, to achieve unsteady evaporation separation by instantaneous heating [3]. The mean free path of a molecule is the average of the distance traveled by a molecule between successive collisions. Molecular distillation equipment has been widely used in the preparation of active ingredients and pharmaceutical intermediates, especially in the separation and purification of high-end pharmaceuticals, cosmetics, nutrition, and other industries [4-8].

The molecular distillation process is generally divided into the following four steps:

(1) Under the action of gravity, centrifugal force, or mechanical stirring, the material forms a continuous and uniform liquid film on the evaporation surface.

(2) The molecules vaporize freely on the surface of the liquid film.

(3) The vapor molecules escaping from the evaporating surface move to the condensing surface.

(4) The light component vapor molecules are condensed when they reach the condensation surface.

†To whom correspondence should be addressed.
E-mail: jmzhang@qust.edu.cn

Kawala and Stephan [9] experimentally found that under the same operating conditions, appropriately increasing the distance between the evaporating surface and the condensing surface, making it larger than the mean free path of the light component molecules, had no significant effect on the separation effect of molecular distillation, but greatly increased the processing capacity. Based on this fact, "molecular distillation" is also proposed as the concept of "short-path distillation", which means that the distance between the evaporating surface and the condensing surface is not limited to the molecular mean free path of the gas. Other studies using molecular distillation test equipment (spacing for 46 mm) and test equipment (spacing for 60 mm) on the medicinal composition in deep-sea fish oil extraction, the heavy phase medicinal components were 29.3% and 30.7%, respectively [10]. The experiments have proved that appropriate increase in the distance between the surface evaporation and condensation surface of molecular distillation separation efficiency has not much impact. However, the mechanism of the physical phenomenon that the distance between heat exchange surfaces has little effect on the separation efficiency has not been explained in detail. In this paper, FLUENT and Molecular Dynamics Simulation were used to discuss the mechanism.

To study the transfer process of molecular distillation in-depth, the molecular distillation process is generally divided into three parts: evaporation, condensation, and gas-phase flow in the transition zone between them. And various corresponding mathematical models are established to explain the mechanism of mass transfer and heat transfer in the molecular distillation process.

The study of gas-phase flow in the transition zone can be modeled from both macroscopically and microscopically. Macroscopic modeling, in which gas is treated as a continuum, uses spatial and

temporal variables of macroscopic flow properties, such as velocity, density, pressure, and temperature. The traditional mathematical model of macroscopic modeling is described by the Navier-Stokes (NS) equation. The microscopic model, also known as the molecular model, regards the gas as composed of numerous discrete molecules, each of which has variables such as position, velocity, and state at any time. The mathematical model at the molecular level is described by the Boltzmann equation.

In the actual molecular distillation unit, the distance between the evaporating surface and the condensing surface is in the same order as the mean free path of gas molecules, so the value of Kn is high and the gas phase flow in the molecular distillation unit is in the transition flow region, which no longer meets the continuum hypothesis. Specifically, when studying the gas flow in molecular distillation, the rarefaction effect of the gas should be considered. The governing equation of the gas flow is the Boltzmann equation:

$$\frac{\partial f}{\partial t}+\xi\frac{\partial f}{\partial x}+\frac{F}{m}\frac{\partial f}{\partial \xi}=\int_{-\infty}^{\infty}\int_{0}^{4\pi}(f^{*}\cdot f_1^{*}-f\cdot f_1)Cr\,\sigma\,d\Omega\,d\xi_1 \quad (1)$$

where $Cr=|\xi_1-\xi|$ is the relative velocity of gas molecules, and has a distribution function $f=f(t, x, \xi)$, $f_1=(t, x, \xi_1)$, $f^{*}=f(t, x, \xi^{*})$, $f_1^{*}=f(t, x, \xi_1^{*})$; velocities ξ^{*} and ξ_1^{*} are the corresponding velocities of two molecules with velocities ξ and ξ_1 when they collide with each other; σ is the molecular pair collision cross section; F is the external force acting on gas molecules; m is the mass of gas molecules; Ω is the solid angle.

In the process of molecular distillation, rarefied gas flow has the characteristics of multi-component, variable temperature, compressibility, and large Kn number. The Boltzmann equation is the best description of the flow problem.

Due to the wide application of short-path distillation in the industrial field, most of the researches focused on the optimization of process conditions, macroscopic liquid film state, and heat transfer [11,12]. There are few researches on the mechanism of molecular distillation from the micro perspective. To better describe the evaporation and condensation process, many scholars at home and abroad have joined the molecular dynamics research at the micro-level to study the heat and mass transfer process at the micro-level [13,14].

To describe the certain transport phenomena in the nonequilibrium transition layer induced by the evaporation, reflection, and condensation of molecules, in the literature [15-17], researchers carry out molecular dynamics (MD) simulations of evaporation and condensation of fluid Ar in a nanochannel. By adjusting the temperature difference (ΔT), between the evaporating and condensing surfaces, they control the steady-state evaporation and condensation fluxes (J_{MD}) [18]. In the evaporation process, the net flux of fluid molecules at the liquid-gas interface is equal to the difference between the molecular flux evaporated from the liquid and the molecular flux condensed on the liquid. The net condensation process is just the opposite.

By changing the length of the nanochannel in the simulation, the molecular number density and temperature were monitored. The temperature and density distribution obtained by molecular simulation was analyzed, and the results show that the mass transfer and heat transfer process is controlled by thermal diffusion, and with the increase of gas-phase length, the convection velocity will eventually exceed the diffusion speed. And the molar fluxes in the gas phase are equal under different lengths, which better explains that there is no resistance in the gas phase process, and the control is realized by convection [17]. Since molecular distillation is a non-equilibrium evaporation condensation process, the evaporation and condensation stage are controlled by diffusion [15,19,20].

At present, most MD models are single-component evaporation and condensation, and there are few studies on multi-component molecular simulation in molecular distillation. To verify the effect of spacing on separation efficiency, the mass and heat transfer simulation of the multi-component distillation process in the transition zone of the evaporative and condensing surface was carried out.

MOLECULAR DYNAMICS SIMULATION

With the development of the application of molecular distillation technology, people have an urgent need to understand the microscopic physical phenomena and physical mechanisms of molecular distillation. Due to the limitation of measurement technology and experimental level, the experimental study on the microscale flow and mass transfer has encountered great difficulties. Therefore, theoretical analysis and simulation have become the main means to study the microscale flow and mass transfer in the gas phase of molecular distillation. In this paper, the flow, mass transfer, and heat transfer of gas components in the transition zone of short-path distillation at the micro-scale were studied by molecular dynamics simulation.

1. Simulation Method

The molecular structure of N-dodecanol and N-hexadecanol is complex. To improve the calculation efficiency, molecular coarse granulation is modeled. Coarse-grained (CG) modeling is an alternative to all-atom (AA) modeling, wherein some of the atomic detail is averaged out so that much longer time and length scales come within reach. In recent years, coarse-grained approaches have been highly successful for a wide range of biomolecular systems such as proteins, lipid bilayers, and carbohydrates [21-24].

In the whole atomic molecular dynamics simulation, the atom is the smallest element of force interaction. The coarse-grained molecular dynamics simulation is based on the whole atom molecular dynamics simulation, which regards several adjacent atoms as a whole, named "beads", as shown in Fig. 1. The coarse-grained model simplifies the molecular structure, reduces the number of degrees of freedom in the simulation, and improves the computational efficiency.

Three molecular simulation systems with different distances are shown in Fig. 2. The space of the bottom 99A * 99A * 99A is composed of liquid molecules. A part of the molecule is fixed as a heating plate, some molecules are also fixed at the top as condensing plates, the thickness of the plate is 40A. The model of the molecular distillation system consists of biphasic molecules: N-dodecanol and N-hexadecanol. The liquid phase at the bottom of the box consists of 1800 N-hexadecanol molecules and 2200 N-dodecanol molecules; the top condensation layer consists of 1500 N-dodecanol molecules. Adjusting the reasonable initial coordinates of atoms

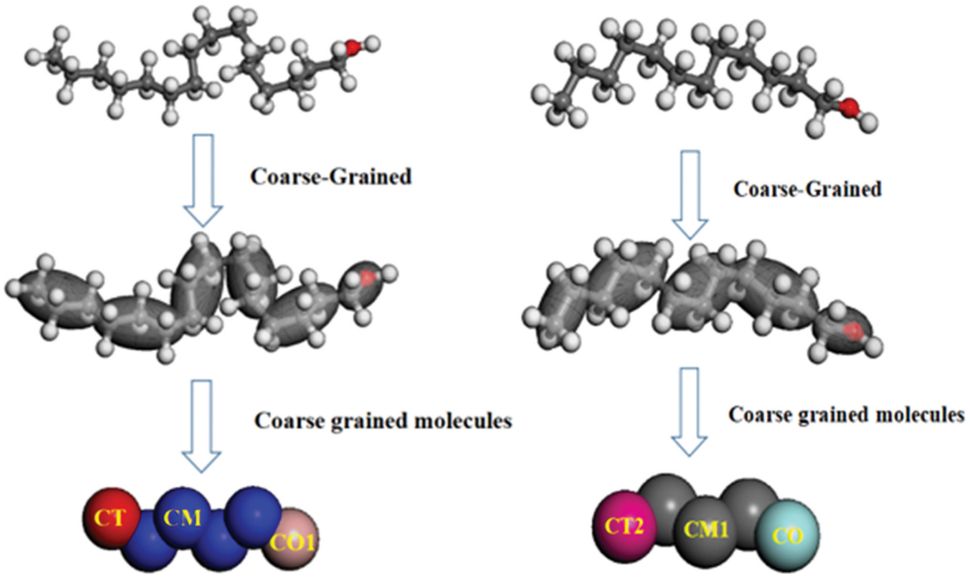

Fig. 1. Coarse-grained molecular model process.

and the energy minimization configuration of the steepest descent algorithm is used [25,26].

Considering the computational efficiency and reasonable reliability under the level of classical mechanics, the molecular group described by L-J potential is used to simulate the actual molecules. The interaction between atoms is described by the L-J potential as follows:

$$\Phi(r_{ij}) = \begin{cases} 4\varepsilon[(\sigma/r_{ij})^{12} - (\sigma/r_{ij})^{6}] & r \le r_{cut} \\ 0 & r > r_{cut} \end{cases} \quad (2)$$

where ε and σ are the energy and distance parameters; r_{ij} is the distance between atoms i and j; r_{cut} is the cut-off radius.

The distance and energy parameters interactions are obtained

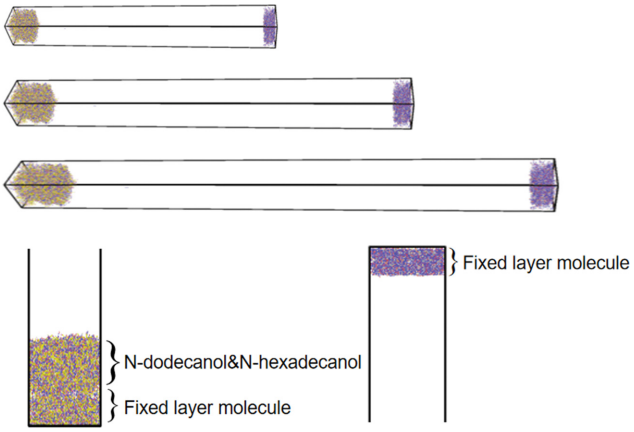

Fig. 2. Initial modeling of the simulation system.

Table 1. Parameters of non-bond stretch potential

Bead-A	Bead-B	D_0 (kcal/mol)	R_0 (A)
CT2	CT2	0.315	4.50
CT2	CM1	0.370	5.02
CT2	CO	0.360	4.50
CT2	CT	0.385	5.01
CT2	CM	0.370	5.02
CT2	CO1	0.360	4.50
CM1	CM1	0.432	5.23
CM1	CO	0.400	4.58
CM1	CT	0.443	5.24
CM1	CM	0.432	5.23
CM1	CO1	0.400	4.58
CO	CO	0.466	4.18
CO	CT	0.430	4.55
CO	CM	0.400	4.58
CO	CO1	0.466	4.18
CT	CT	0.470	5.22
CT	CM	0.443	5.24
CT	CO1	0.430	4.55
CM	CM	0.432	5.23
CM	CO1	0.400	4.58
CO1	CO1	0.466	4.18

Note: D_0 is the well depth of potential, and R_0 is the equilibrium distance.

Table 2. Parameters of bond stretch potential

Bead-A	Bead-B	K_b (kcal/mol/A^2)	R_0 (A)
CT2	CM1	22.11	3.14
CM1	CM1	15.65	3.72
CM1	CO	15.76	3.02
CT	CM	13.93	3.73
CM	CM	15.65	3.72
CM	CO	15.76	3.02

Note: K_b is the bond force constant, and R_0 is the equilibrium distance.

Table 3. Parameters of angle bend potential

Bead-A	Bead-B	Bead-C	K_0 (kcal/mol/rad^2)	θ_0 (degree)
CT2	CM1	CM1	7.81	156
CM1	CM1	CM1	8.59	153
CM1	CM1	CO	5.86	151
CT	CM	CM	5.97	149
CM	CM	CM	8.59	153
CM	CM	CO	5.86	157

Note: K_0 is the bond angular force constant, and θ_0 is the equilibrium angle.

according to the Lorentz-Berthelot combining rules, as follows:

$$\sigma_{A-B}=(\sigma_{A-A}+\sigma_{B-B})/2 \quad (3)$$

$$\varepsilon_{A-B}=\sqrt{\varepsilon_{A-A}\cdot\varepsilon_{B-B}} \quad (4)$$

where ε and σ are the energy and distance parameters; the subscripts A and B represent different atom types.

The L-J potential parameters [27] are listed in Tables 1-3. Moreover, r_{cut}=1.20 nm is the overall cutoff distance for the L-J potential.

As shown in Fig. 3, the system uses three-dimensional periodic

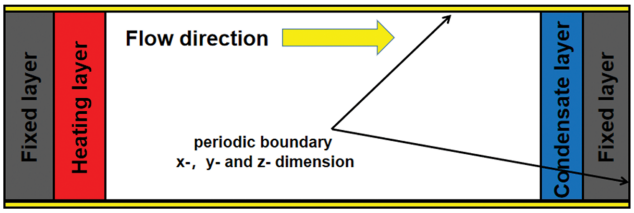

Fig. 3. The position and boundary of the structure of each part in the simulation system.

boundary conditions. The simulation consists of two independent ensembles, named NPT, NVE-Langevin. NPT part equilibrates the system to 0.75 ns in a vacuum environment of 298 K; this command performs time integrals on the Nose-Hoover form of the non-Hamiltonian equation [26]. A Nose-Hoover thermostat will not work well for arbitrary values of Tdamp. If Tdamp is too small, the temperature can fluctuate wildly; if it is too large, the temperature will take a very long time to equilibrate. A good choice for many models is a Tdamp of around 100 timesteps and a Pdamp of around 1,000 timesteps. The NVE ensemble is used to apply the Langevin thermostat to the molecular group. The command performs Brownian kinematics (BD) and the total force acting on

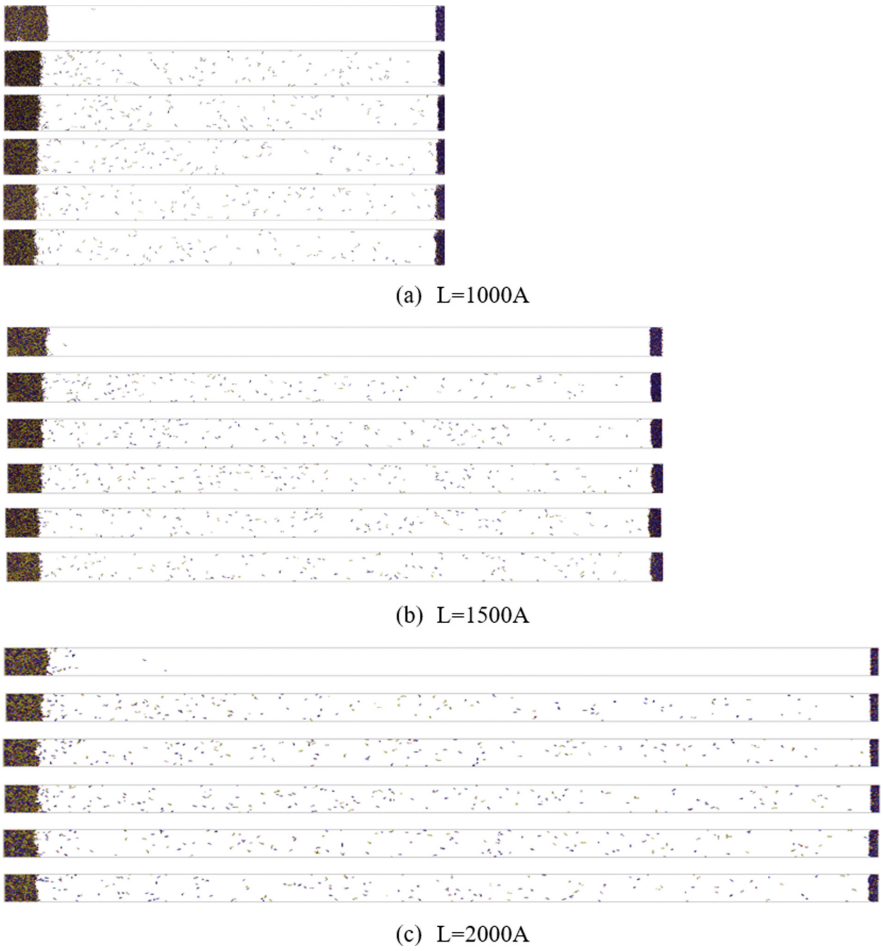

Fig. 4. The material distribution in the process of mass transfer and heat transfer in molecular distillation at distances of 1000A,1500A, and 2000A respectively.

each atom is:

$$F = F_c + F_f + F_r \quad (5)$$

$$F_f = -(m/damp)\upsilon \quad (6)$$

$$F_r = \sqrt{(k_b \cdot mT)/(damp \cdot \delta t)} \quad (7)$$

where F_c is the conservative force computed via the usual inter-particle interactions; F_f is a frictional drag or viscous damping term proportional to the particle's velocity; F_r is a force due to solvent atoms at a temperature T randomly bumping into the particle; m is the mass of the particle; damp is the damping factor specified by the user; υ is the relative velocity of particles; K_b is the Boltzmann constant; T is the desired temperature; δt is the timestep size.

And the proportionality constant for each atom is computed as m/damp. As derived from the fluctuation/dissipation theorem, its magnitude, as shown above, is proportional to $\sqrt{(k_b \cdot mT)/(damp \cdot \delta t)}$. The data sampling interval in the NVE section is 1,000 fs, the whole period is 10 ns.

The evaporation of molecules is caused by the sudden increase in the temperature of the specific fixed molecules at the bottom. The temperature of the bottom heating layer is set at 540 k, and the temperature of the top condensation layer is set at 293 K. To better illustrate the molecular distillation process, the atomic distribution at different time points is shown in Fig. 4. Compared with the reflective boundary layer, the condensation layer can avoid the rebound of molecules when they reach the fixed layer, which greatly slows the collision between molecules [26]. In this paper, the main factors of mass and heat transfer in the transition region are discussed by analyzing the molecular temperature and density in the transition region.

2. Data Analysis

To better explain the influence of the change of heat exchange surface spacing on molecular distillation efficiency, under the premise of keeping the evaporation temperature (500 K) and condensation temperature (293 K) unchanged, the evaporation efficiency with the spacing of 1000A, 1500A, and 2000A was calculated, respectively, and the results are shown in Fig. 5. Through sampling at different time points, we can find that the molecular distillation efficiency is maintained at about 88%-91% under the three groups of spacing, which verifies that the change of spacing does not have a significant impact on the separation efficiency, consistent with previous experiments [9].

As shown in Fig. 6(a), the molecular number density and temperature with a spacing of 1000A are analyzed. We find that the data near the bottom and top fluctuate violently, and the data in the middle region change gently. That is, the mass and heat transfer in the evaporation and condensation stage of molecular distillation is in an unstable state, and the mass and heat transfer in the transition region reaches a steady equilibrium. Molecules in the evaporation region constantly absorb heat, and different molecules need different energy for evaporation, which leads to the existence of a velocity gradient between molecules. Therefore, in the evaporation stage, the molecules are in an unstable state and the temperature fluctuates violently. The evaporated molecules collide with each other, making the energy difference between molecules into the mean velocity, that is, the molecules in the transition zone are in a stable

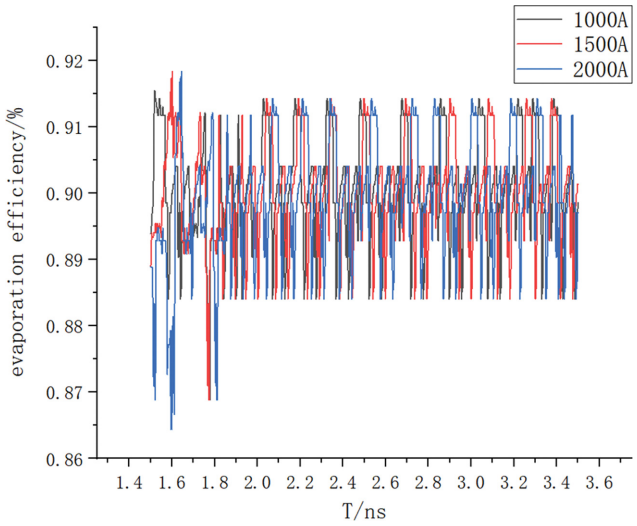

Fig. 5. Evaporation efficiency at different time when spacing is 1000A, 1500A and 2000A.

state, the temperature is in a state of equilibrium, and the distribution of molecules is relatively uniform.

To further verify the influence of heat transfer surface distance on the mass and heat transfer process of molecular distillation, simulation analysis was conducted on the models with spacing of 1500A and 2000A, respectively, and the results are shown in Fig. 6(b) and (c). The data show that the mass transfer and heat transfer in the molecular distillation process do not change with the increase of the distance between the heat transfer surface. The temperature and density in the evaporation and condensation stage fluctuate violently and are in an unstable state. The mass and heat transfer in the transition zone is in a stable state.

From the above data analysis, we can conclude that in the process of molecular distillation, the mass and heat transfer of evaporation and condensation is controlled by heat diffusion, which will produce violent fluctuations; the mass and heat transfer process in the transition zone is controlled by convection and in dynamic equilibrium. At the same time, it is verified that the distance does not affect the mass transfer and heat transfer process, that is, it has little effect on the distillation efficiency of the molecular distillation process.

3. Results Analysis

Molecular dynamics simulation of short-range distillation was carried out:

(1) In the distillation process, the stability and molecular density near the evaporation condensation end fluctuate greatly, which belongs to unsteady heat and mass transfer;

(2) The temperature and density in the transition zone between the evaporation surface and condensation surface have no fluctuation and are in a stable range.

NUMERICAL SIMULATION OF THE TRANSITION ZONE

1. Modeling

The volume fraction and temperature change of the gas and liq-

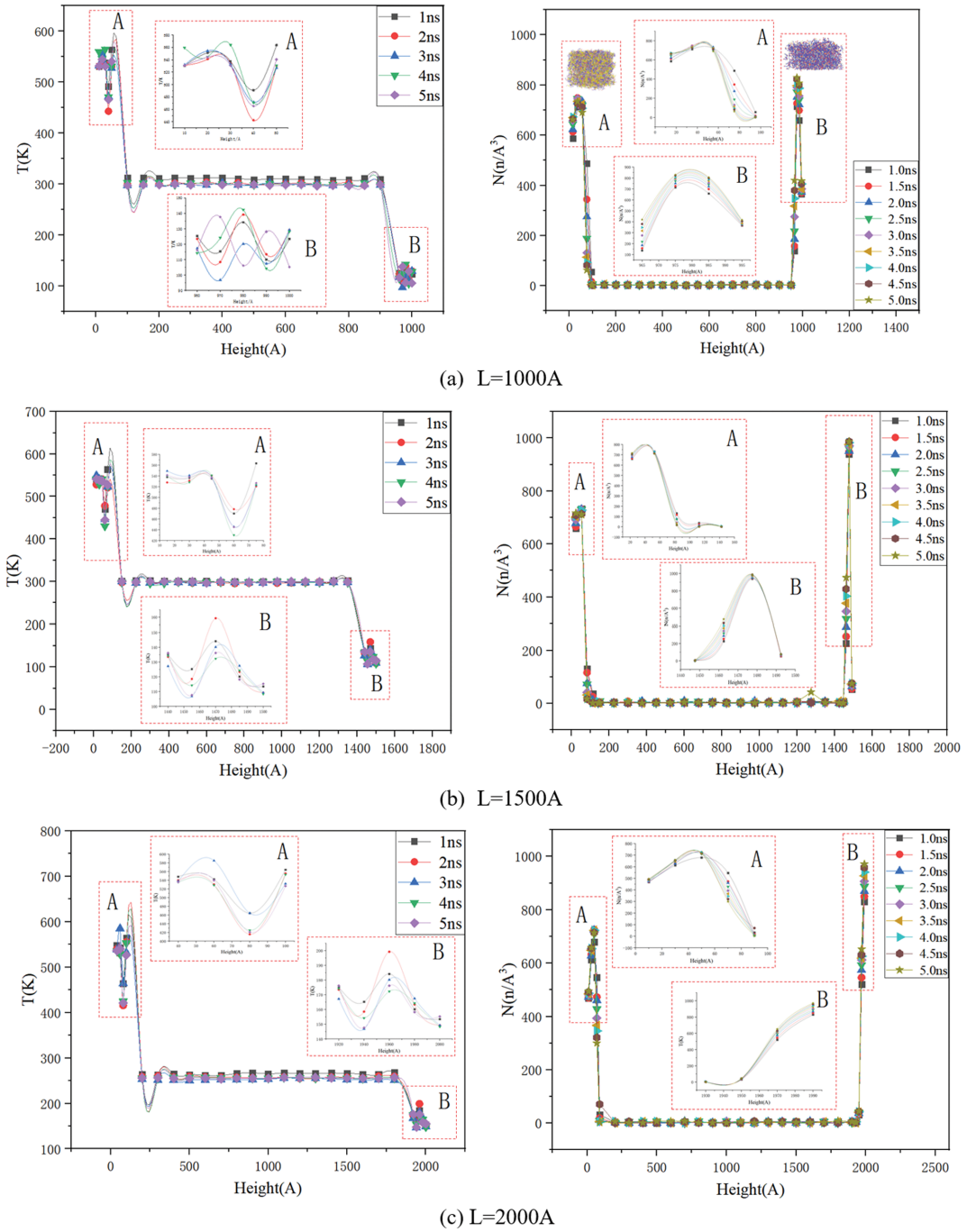

Fig. 6. Distribution of temperature and density curves of molecular distillation during mass transfer and heat transfer at a distance of 1000A, 1500A and 2000A.

uid phases in the transition zone of short-path distillation are the main reference quantities reflecting the state of the transition zone. To compare the influence of the distance between the hot and cold surfaces on the parameters of the transition zone, ICEM-CFD was used to establish a simplified two-dimensional simplified model of the short-path distillation device. A two-dimensional grid model of the longitudinal section of evaporation and condensation is shown in Fig. 7. Except for the distance between the hot and cold surfaces of the model (10 mm, 20 mm, 40 mm), the other parameter settings are the same. In ICEM-CFD, the unstructured grid is divided and the boundary conditions are refined. The number of grids is 158,039, 184,253 and 215,689. After the grid independence test (Fig. 8), the number of selected grids meets the calculation requirements.

2. Condition Setting

To simplify the calculation process, two assumptions were made for the calculation model: (1) Air and liquid do not dissolve each other; and (2) the computational fluid is incompressible. The physi-

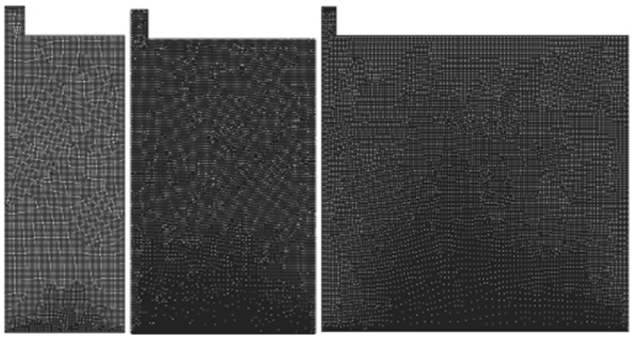

Fig. 7. 2D model grid.

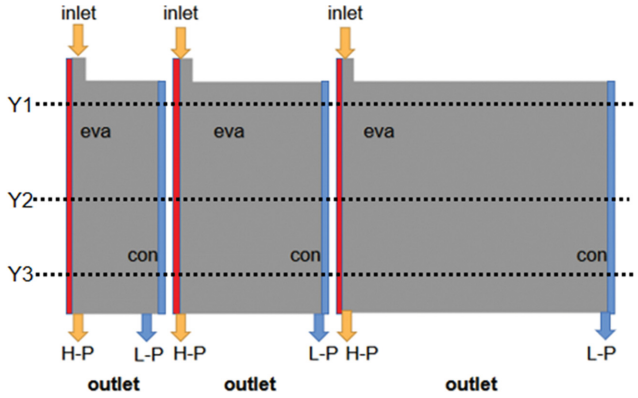

Fig. 9. The division of flow field for 2D.

cal parameters of the research object are shown in Table 4 [28]. The shape of the liquid-gas interface changes with flow time and the VOF model was used to track this change, with air as the main phase, N-hexadecanol and N-dodecanol as the liquid phase, and N-dodecanol vapor as the forming phase. The energy equation was activated and the turbulence model was selected as the RNG k~ε model.

To fully describe the heat and mass transfer in the evaporation and condensation region, three monitoring lines were selected in the longitudinal direction with equal spacing (10 mm) to monitor the upper end, middle end and lower end of the mixed liquid phase, respectively, as shown in Fig. 9.

Uncoupled solution, implicit algorithm, and steady-state process are selected for calculation. The momentum equation adopts the second-order upwind discrete scheme, the pressure and velocity correlation adopts the PISO method. The convergence accuracy of the residual error of the momentum equation and the continuity equation is set as 1e-05. Operation was at atmospheric pressure, the gravity option was activated, and the gravitational acceleration was 9.81 m/s^2.

3. Simulation Result

By monitoring the phase volume fraction and temperature change on the Y1Y2Y3 line, the material transfer process in the short-range distillation transition zone is determined.

3-1. Change Trend of Gas and Liquid Volume Concentration

After the mixture enters the heating surface with steady speed, the light components are heated and vaporized into N-dodecanol gas, and the vapor condenses into a liquid on a condensing surface by irregular motion. To compare the influence of different evaporation plane spacing, the vapor and liquid phase distribution data curves of the three observation lines Y1-Y3 for the evaporation and condensation sections of L=10 mm, L=20 mm and L=40 mm are shown in Fig. 10.

According to the movement trend of the integral number of gas and liquid in the evaporation area, it can be simplified into three states. In the Y1-Y3 reference line gas-liquid volume fraction change curve of the three models (Fig. 11): the first stage is the violent evaporation stage, which evaporates rapidly on the evaporation surface, and the light component is vaporized by heat, and a large

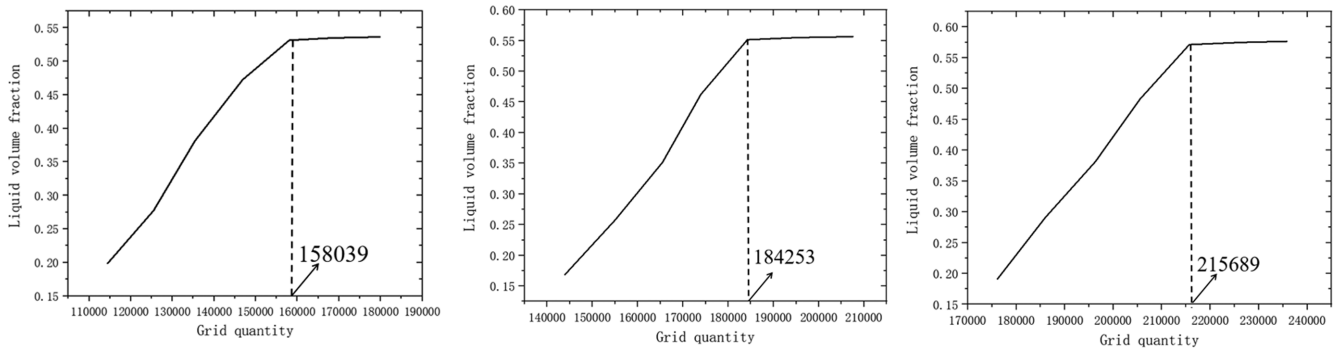

(a) L=10mm (b) L=20mm (c) L=40mm

Fig. 8. Grid independence validation.

Table 4. Physical parameters of research object

Name	ρ kg/m^3	C j/(kg·K)	η kg/(m·s)	M_r	M.P/K	B.P/K
N-hexadecanol	817.6	3,433.349	1.79	242.44	322.35	617.65
N-dodecanol	831	3,623.58	1.15	186.34	196.95	536.95

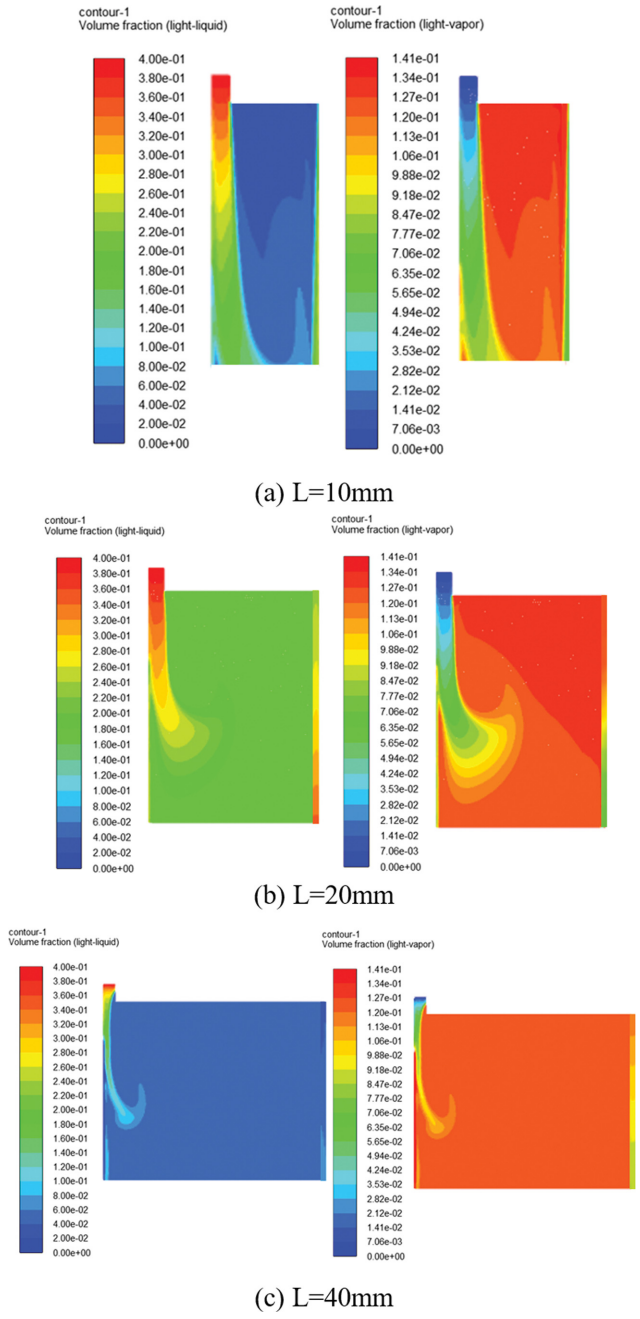

(a) L=10mm

(b) L=20mm

(c) L=40mm

Fig. 10. Gas-liquid distributions cloud map with spacing of 10 mm, 20 mm and 40 mm.

amount of steam escapes from the liquid level. The evaporation stage is more pronounced at Y1 near the entrance, and the evaporation phenomenon is violent. In Y2 and Y3 lines, the content of light components decreases, and the evaporation phenomenon is not obvious. The second stage is the stable transition zone, which is dominated by the gas phase. After leaving the liquid level, the concentration of gas-phase reaches a peak quickly and then enters a stable state. In terms of gas-liquid state parameters in the transition zone, the three models are the same, which is not affected by the distance of evaporation and condensation. The variation trend of the gas phase in the transition region is highly consistent between the three models, and it is a stable state of mass transfer. The third stage is the gas phase condensation stage. After passing through the transition zone, a large number of molecules of gas-phase gather on the condensing surface. A small number of light components condense into the liquid phase, and the fluctuation of gas-phase volume fraction decreases (Fig. 10). The phase volume fraction of the three models under the three monitoring lines is surprisingly consistent. The decrease of the gas phase and the increase of a small amount of the liquid phase conform to the principle of condensation (Fig. 11).

3-2. Change Trend of Gas and Liquid Temperature

By preheating, the material is heated to 300 K to increase fluidity. We set the heating temperature at 450 K and the condensation temperature at 273 K. The cloud chart of temperature in the short-path distillation evaporation condensation zone is shown in Fig. 12. The temperature variation trend of the three models was consistent, the liquid phase in the heating region was heated at a faster rate, and the temperature gradient was not obvious. The temperature in the transition zone was constant and did not fluctuate, and the temperature before and after the condensation zone shows an obvious gradient space.

In the initial feeding stage, the liquid phase evaporates quickly when heated, and the temperature of the gas and liquid phase rises at the upper end. After the feed is stable, it can be seen from Fig. 13 that the temperature near the evaporation surface is higher. The temperature of the three models is stable at 310-320 K in the middle section. In the condensation stage, the temperature shows a significant downward trend, and there is a small peak in the temperature near the condensation surface, which is caused by the heat release of water vapor condensation. It can be seen from the temperature change trend of the cloud diagram and the graph that in the intermediate stage of short-path distillation, due to the effect of convection and mass transfer, the temperature is stable and without fluctuation in the transition zone; in the condensation stage, due to the exothermic heat of the heat transfer process, the temperature rises slightly after falling.

4. Results Analysis

From the Fluent simulation, the data of vapor phase transfer at evaporation condensation interface with different spacing are summarized as follows:

(1) On the evaporation wall, the light phase material is evaporated into gas by heating, and the gas-liquid phase is separated. The temperature rises rapidly and shows a fluctuating downward trend after reaching the boiling point.

(2) In the process of approaching the condensing surface, the molecular volume fraction of the light phase decreases, the volume fraction of the liquid phase increases gradually, and there is slight fluctuation. The temperature has slight heat release during liquefaction and decreases to the temperature of the condensation surface.

(3) The volume fraction and temperature of the gas-liquid phase are stable in the transition region, which belongs to the category of convective mass transfer. There is no significant difference in the state of the transition zone when the spacing changes. This is consistent with the previous experimental results [9,10], that the increase of spacing has little effect on the separation efficiency.

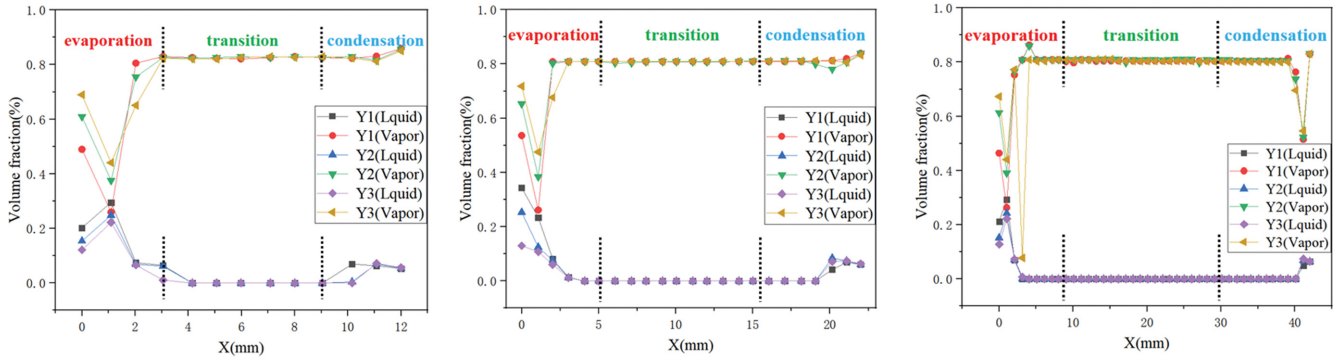

(a) L=10mm (b) L=20mm (c) L=40mm

Fig. 11. Gas-liquid distribution curves with spacing of 10 mm, 20 mm and 40 mm.

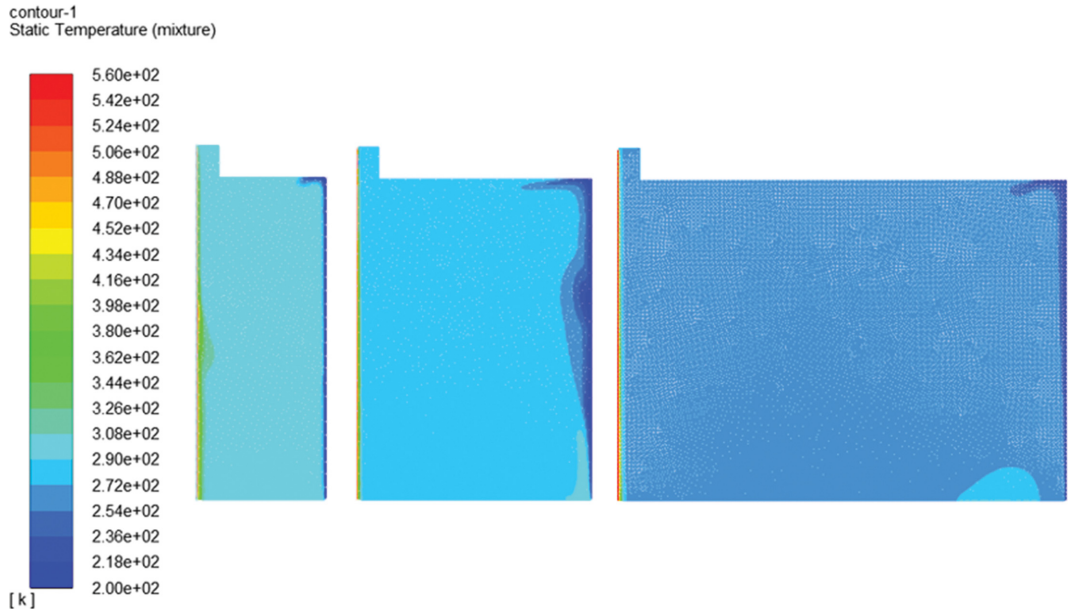

Fig. 12. Temperature distributions cloud map with spacing of 10 mm, 20 mm and 40 mm.

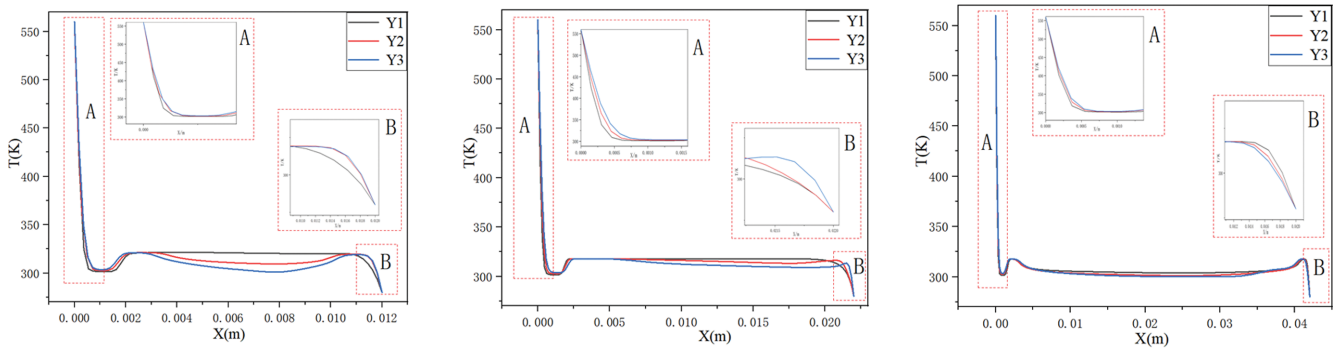

(a) L=10mm (b) L=20mm (c) L=40mm

Fig. 13. Temperature distribution curves with spacing of 10 mm, 20 mm and 40 mm.

CONCLUSION

Molecular dynamics simulation was introduced into the study of the micro mechanism of the distillation process and heat and mass transfer process in short-range distillation equipment. However, there is sometimes a big difference between the rule of the

micro and the macro, so CFD simulation was used to simulate the macroscopic process. Fluent and molecular simulation software were combined to analyze the transition region of the gas-phase transfer process.

The heat and mass transfer in the transition zone between evaporation and condensation surfaces of short-range distillation was studied by Fluent and molecular simulation. By simulating the transition zone between the evaporation and condensation surfaces, it was found that the temperature and molecular density in the gas phase are unchanged through the simulation of steady-state evaporation and condensation of molecules. That is, the heat and mass transfer in the gas phase is mainly controlled by convection rather than the diffusion process. While in the study of transient heat and mass transfer dynamics between cold and hot surfaces, the mass and heat transfer in steam is controlled by thermal diffusion. It is verified that in short-path distillation, the distance between the hot and cold surfaces has no significant effect on evaporation and condensation. According to the result, we can zoom in very nicely on the molecular distillation apparatus. Increasing the distance between the evaporation surface and the condensation surface does not affect the separation efficiency, and can greatly reduce the difficulty of manufacturing. In addition, the increase of the distance between the evaporation surface and the condensation surface increases the volume capacity of the transition zone, which can provide more location space for the evaporated materials. The processing capacity of the materials is greatly increased, and the production capacity in the industrial production is improved.

ACKNOWLEDGEMENT

This work was supported by a grant from the Shandong Province Taishan Scholar engineering under special funding Foundations, Shandong Provincial Natural Science Foundation (ZR2020MB122), and the Tackling Key Program of Science and Technology in Shandong Province (No. 2019GSF109009; No. 2017GGX40113).

SYMBOL DESCRIPTION

$c_r = \xi_1 - \xi$: the relative velocity of gas molecules
ξ^*, ξ_1^* : the corresponding velocities of two molecules with velocities ξ and ξ_1 when they collide with each other
σ : the molecular pair collision cross section
F : the external forces acting on gas molecules
m : the mass of gas molecules
Ω : the solid angle
ε : energy parameters
r_{ij} : the distance between atoms i and j
r_{cut} : the cut-off radius
A, B : represent different atom types
F_c : the conservative force computed via the usual inter-particle interactions
F_f : a frictional drag or viscous damping term proportional to the particle's velocity
F_r : a force due to solvent atoms at a temperature T randomly bumping into the particle
damp : the damping factor specified by the user
υ : the relative velocity of particles
K_b : the Boltzmann constant
T : the desired temperature
δ_t : the timestep size

REFERENCES

1. J. Fu, X. Han, J. Hu, W. Xiong and L. Wu, *The Food Ind.*, **41**(09), 186 (2020).
2. G. Zhao, Y. Zhao, L. Lu and Z. Hou, *Special Wild Economic Animal and Plant Research*, **42**(03), 53 (2020).
3. T. Xu and W. Han, *Mech. Electr. Inform.*, **3**(08), 1 (2015).
4. H. Dong and R. Wang, *Chem. Design Commun.*, **45**(03), 55 (2019).
5. X. Sun, *Technol. Dev. Chem. Ind.*, **47**(12), 35 (2018).
6. G. Zhu, *Petrolem Prod Appucation Res.*, **36**(05), 76 (2018).
7. Y. Tao, C. Li, W. Wu and Y. Gao, *Sci. Technol. Food Ind.*, **33**(03), 429 (2012).
8. Y. Li and J. Liu, *Cereals Oils*, **1**(03), 7 (2011).
9. Z. Kawala and K. Stephan, *Chem. Eng. Technol.*, **12**(1), 406 (1989).
10. Y. Ren, Tianjin Univ (2006).
11. J. Guo, S. Su, H. Li, S. Han and D. Qian, *Mod. Chinese Med.*, **15**(01), 9 (2013).
12. H. Li, Y. Li, C. Hu and J. Han, *Res. Explor. Lab.*, **31**(07), 54 (2012).
13. A. H. Persad and C. A. Ward, *Chem. Rev.*, **116**(14), 7727 (2016).
14. D. J. Henry, V. I. Dewan and E. L. Prime, *J. Phys. Chem. B*, **114**(11), 3869 (2010).
15. Z. Liang and P. Keblinski, *The J. Chem. Phys.*, **148**(6), 064708 (2018).
16. Z. Liang, T. Biben and P. Keblinski, *Int. J. Heat Mass Tran*, **114**, 105 (2017).
17. Z. Liang, A. Chandra, E. Bird and P. Keblinski, *Int. J. Heat Mass Tran.*, **149**, 119 (2020).
18. Z. Wang, Tsinghua Univ (2002).
19. Y. Gu, S. Ge and M. Chen, *Mol. Phys.*, **114**(12), 1922 (2016).
20. S. Ge, Y. Gu and M. Chen, *Mol. Phys.*, **113**(7), 703 (2015).
21. R. Kumar, Y. K. Lee and Y. S. Jho, *Int. J. Mol. Sci.*, **21**(13), 4602 (2020).
22. J. Roel-Touris and A. M. J. J. Bonvin, *Comput. Struct. Biotec.*, **18**, 1182 (2020).
23. T. A. Beu, A. E. Ailenei and R. I. Costinaş, *J. Comput. Chem.*, **41**(4), 349 (2020).
24. A. T. Shivgan, J. K. Marzinek and R. G. Huber, *J. Chem. Inf. Model*, **60**(8), 3864 (2020).
25. Y. Tang, X. Zhang, Y. Lin, J. Xue, Y. He and L. Ma, *Adv. Theor. Simul.*, **2**(8), 1900065 (2019).
26. C. Qun, S. Wei and C. Zheng, *Int. J. Heat Mass Tran.*, **153**, 119616 (2020).
27. P. Wang, China Univ Petroleum (East China) (2013).
28. H. Xing, *J. Wuhan Inst. Chem. Technol.*, **27**(01), 72 (2005).